

## Article

# Improvement of Microstructure and Sliding Wear Property of Cold-Sprayed FeAl Intermetallic Compound Coating by Annealing Treatment

Hongtao Wang <sup>1,2,\*</sup>, Fenghui An <sup>1,2</sup>, Xiaobo Bai <sup>1</sup>, Hailong Yao <sup>1,2</sup>, Mengxian Zhang <sup>1,2</sup>, Qinyu Chen <sup>1</sup>, Gangchang Ji <sup>1,2</sup> and Chidambaram Seshadri Ramachandran <sup>3,\*</sup>

<sup>1</sup> School of Material Science and Engineering, Jiujiang University, Jiujiang 332005, China

<sup>2</sup> Jiangxi Province Engineering Research Center of Materials Surface Enhancing & Remanufacturing, Jiujiang 332005, China

<sup>3</sup> Department of Materials Science and Engineering, The State University of New York at Stony Brook, New York, NY 11794, USA

\* Correspondence: wanght7610@163.com (H.W.); csrnc1@gmail.com (C.S.R.)

**Abstract:** Nanograin Fe(Al) solid solution alloy coating was firstly produced through cold-spraying technology using mechanically alloyed powder. Then, the above-mentioned coating was annealed at different temperatures to explore its influence on the phase constitution, microstructure, microhardness and dry sliding wear property of the coatings. Results exhibited that an FeAl phase appeared in the coatings after 500 °C treatment and remained stable with increasing annealing temperature. The annealing temperature had a considerable effect on the microstructure, microhardness and wear behavior of the FeAl coating. The existing laminated structure in the as-sprayed coating gradually faded away with increasing temperature and finally obtained a dense coating microstructure with no particle interface when annealed above 950 °C. Nanograin began to evidently grow at temperatures over 800 °C. The microhardness of the FeAl coating stayed at 400 Hv<sub>0.1</sub> at temperatures below 800 °C, then it quickly dropped to 300 Hv<sub>0.1</sub> at 950 °C and remained nearly unchangeable up to 1100 °C. The dry sliding wear mechanism of the FeAl coating annealed at low temperatures below 700 °C was mainly delamination of the oxide layer and showed a high wear rate within the order of magnitude range of 10<sup>-4</sup>, whereas FeAl coatings annealed at high temperatures above 950 °C were worn by microploughing and little oxidation and exhibited very low wear rates within the order of magnitude range of 10<sup>-6</sup>.

**Keywords:** cold spraying; FeAl coating; microstructure; microhardness and wear property; annealing treatment



**Citation:** Wang, H.; An, F.; Bai, X.; Yao, H.; Zhang, M.; Chen, Q.; Ji, G.; Ramachandran, C.S. Improvement of Microstructure and Sliding Wear Property of Cold-Sprayed FeAl Intermetallic Compound Coating by Annealing Treatment. *Coatings* **2023**, *13*, 1260. <https://doi.org/10.3390/coatings13071260>

Academic Editor: Robert B. Heimann

Received: 15 June 2023

Revised: 11 July 2023

Accepted: 16 July 2023

Published: 18 July 2023



**Copyright:** © 2023 by the authors. Licensee MDPI, Basel, Switzerland. This article is an open access article distributed under the terms and conditions of the Creative Commons Attribution (CC BY) license (<https://creativecommons.org/licenses/by/4.0/>).

## 1. Introduction

FeAl intermetallic alloys possess advantageous properties such as high melting points, low cost and density, high intermediate temperature strength and remarkable corrosion resistance in hostile atmospheres [1,2]. Therefore, FeAl intermetallics have good potential for structural applications in heat treating, automotive, steel-making and fossil energy industries acting as heating elements, furnace fixtures, and piping [2–5]. However, the poor ambient temperature ductility and insufficient creep strength of FeAl alloy limits its wide industrial application [2]. A nanocrystalline structure obtained by mechanical alloying was found to significantly improve the ductility of intermetallics [6]. Consequently, FeAl structural materials with even a small nanograin have attracted much more interest. Thermal spray processes have been used to fabricate nanostructured intermetallic coatings by spraying ball-milled intermetallic feedstocks [7–9]. However, high temperatures during spraying would change the pre-designed phase structure, chemical composition and microstructure of feedstocks and consequently worsen the coating performance.

In the past decades, cold spraying (or cold gas-dynamic spraying) has evolved expectations for the fabrication of nanocrystalline materials tremendously. In this process, deposited particles always keep their solid state due to the low spraying temperature (far below the melting point of the feedstock material). A coating is formed through the intensive plastic deformation of flying particles upon impact on the substrate and pre-deposited particles [10]. The low-temperature characteristic and high deposition rate make cold spraying an efficient process to deposit metals [11–13], composites [14–16] and even cermet materials [17–19] with a limited influence on the microstructure of feedstocks. As a result, the cold spraying process was expected to be a potential process to employ in the deposition of nanostructured FeAl coating. Our previous study has shown that the nanostructured FeAl intermetallic [20] and FeAl/Al<sub>2</sub>O<sub>3</sub> composite [21] coatings can be prepared through cold-spray depositing of the milled powders, followed by annealing treatment.

Generally, coating microstructure has a significant influence on the properties of coatings. As far as cold-sprayed coating is concerned, the inter-particle bonding strength is low because of its mechanical bonding feature, which can lead to a heterogeneous microstructure and consequently, poor mechanical strength [22]. Many studies have indicated the significant effect of a post-spray annealing treatment on cold-sprayed coating properties [22–26]. Our previous study [27] also found that the erosion resistance of cold-sprayed FeAl coatings can be substantially enhanced after annealing treatment at 950 °C, which was superior to that of heat-resistant 2520 stainless steel bulk material by a factor of three under an abrasive temperature of 800 °C. Therefore, the annealing treatment may provide an approach to modify the microstructure and properties of cold-spray nanostructured FeAl coatings. However, nanograin FeAl has lower thermal stability; therefore, nanograin growth would occur alongside microstructure improvement during the annealing treatment, which would decrease coating properties such as microhardness and wear property [28].

Therefore, the effect of annealing temperature on the microstructure and property evolution of cold-sprayed FeAl coating was investigated in this paper. Modification of phase structure, grain size and microstructure were observed, microhardness and sliding wear property were tested, and the relationship between coating microstructure and mechanical properties was also examined.

## 2. Experimental Materials and Procedures

### 2.1. Materials

In this study, commercially available Fe (~54 µm, 99.8 wt.%) and Al (~74 µm, 99.5 wt.%) powders were provided by Youxinglian Nonferrous Metals Ltd., Beijing, China. An Fe-40Al (at.%) powder mixture was fabricated using the above-mentioned Fe and Al powder. The mechanical alloying of Fe(Al) solid solution alloy powder was processed using a high-energy ball mill (ND-4L, Nanjing University, Nanjing, China) for 36 h under an argon atmosphere. The details of this experimental step have been described elsewhere [20]. After ball milling, the sieved Fe(Al) alloy powder (~30 µm) was used as feedstock for spraying. SEM images of surface and cross-section morphology of milled Fe(Al) powder are shown in Figure 1. The milled powder presented an irregular morphology due to the continuous impacting, cold-welding and fracturing effect during the mechanical alloy process. It was noticeable that many small, laminated structures existed in the inner part of the milled powder (as shown in Figure 1b), which indicated an inhomogeneous microstructure and composition.

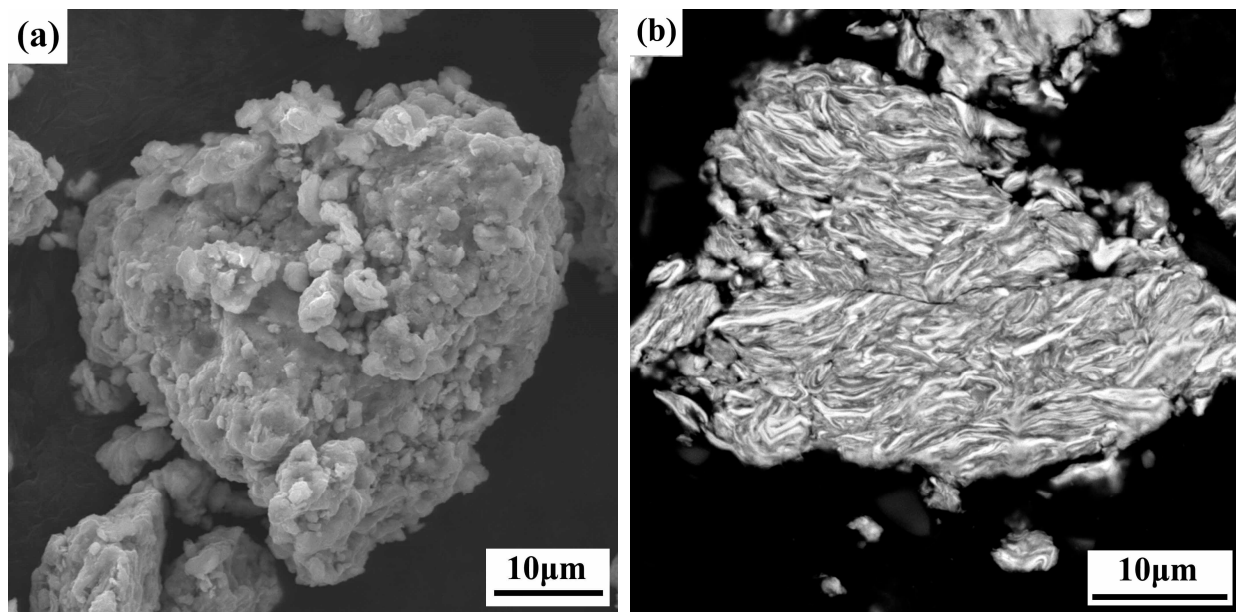


**Figure 1.** SEM images of surface (a) and cross-section morphologies (b) of the feedstock for cold spraying.

### 2.2. Coating Deposition and Annealing Treatment

Coatings were prepared using a laboratory-made cold spray system. Detailed information about this spray equipment has been described previously [13]. The de Laval-type nozzle is 100 mm in length with a throat and exit diameter of 2 mm and 6 mm, respectively. During the deposition process, heated nitrogen gas was used both as the propelling gas and the particle-carrying gas. The detailed parameters used in the cold spray process are shown in Table 1. Substrate specimens were stainless steel plates (1Cr18Ni9Ti) with the dimensions of 50 × 50 × 5 mm. The plate surface was degreased with acetone and sand blasted using brown corundum grits prior to spraying.

**Table 1.** Processing parameters in cold spraying.

Spraying Parameters	Value
Accelerating gas	N <sub>2</sub>
Powder carrying gas	N <sub>2</sub>
Accelerating gas pressure/MPa	2.0
Powders carrying gas pressure/MPa	2.5
Accelerating gas temperature/°C	500
Gun traverse speed over substrate/mm/s	40
Standoff distance/mm	20

Following cold spraying, as-sprayed coating samples were annealed for different times at temperatures of up to 1100 °C in a furnace under an argon atmosphere.

### 2.3. Coating Characterization and Wear Test

The phase and microstructure evolution of FeAl coatings was examined using an X-ray diffraction diffractometer (XRD, XRD-6000, Shimadzu, Kyoto, Japan) and scanning electron microscopy (SEM, Quanta 200, FEI, Czechoslovakia) equipped with energy dispersive X-ray analysis (EDS), respectively. The grain size and morphology of FeAl coatings after annealing were also investigated by transmission electron microscope (TEM, JEM-200CX, JEOL, Japan). A Vickers microhardness tester (HVS-1000, Shanghai Cany Precision Instrument Co., Ltd., Shanghai, China) was used to measure the hardness of coatings under a 100 g load, averaging the results of 10 measurements.

The wear property of as-sprayed Fe(Al) alloy coating and annealed FeAl coatings treated at 700 °C, 950 °C and 1050 °C for 5 h were evaluated using a dry sliding test in a ball-on-plate tribotester (Model: CFT-I, manufacturer: Lanzhou Zhongke Kaihua Technology Development Co., Ltd., China) at room temperature. Prior to testing, coating samples with dimensions of 10 × 10 × 5 mm were ground and metallographically polished to obtain a smooth surface with an average roughness (Ra) between 0.4 and 0.8 μm, followed by ultrasonic cleaning in acetone for 10 min and drying in air. The counterpart was an Si<sub>3</sub>N<sub>4</sub> ceramic ball of 6 mm diameter (hardness about HRC90) with a surface roughness of 0.01 μm. During tests, the Si<sub>3</sub>N<sub>4</sub> ceramic ball was kept stationary and coating samples kept reciprocating movement. The sliding velocity and testing load were 50 mm/s and 10 N, respectively. The sliding amplitude was 5 mm, and the total wear time was 30 min for one test (calculated wear distance: 90 m). The friction coefficient change curve was automatically recorded. After the wear test, the worn morphology was measured using a surface profilometer and wear width and wear volume could be obtained. Wear rate was calculated by dividing the wear groove volume by the sliding distance and applied load. Three replicate tests were conducted for each run of tests and the averaged wear data were given. The worn surface morphology of the coating samples was investigated by SEM and wear failure mechanisms responsible for the sliding wear process were analyzed in detail.

### 3. Results and Discussion

#### 3.1. Microstructure Characterization of the As-Sprayed Coating

SEM images of the microstructure of the as-sprayed coating are shown Figure 2. Apart from a great deal of refined lamellar structure, a trace of white layers of considerable thickness can also be found in the coating, as shown in Figure 2b. In order to investigate the chemical constitute of the above-mentioned area, three different zones in Figure 2b, namely A, B and C zones were measured using EDS. On the basis of EDS analysis (as shown in Table 2), these white layer region was an Fe-rich Fe(Al) solid solution phase and the fine lamella region was an Al-rich Fe(Al) phase. It is necessary to point out that this lamellar structure comes from both the inner layer of deposited particles and the inter-particle interface, as shown in Figure 1b.

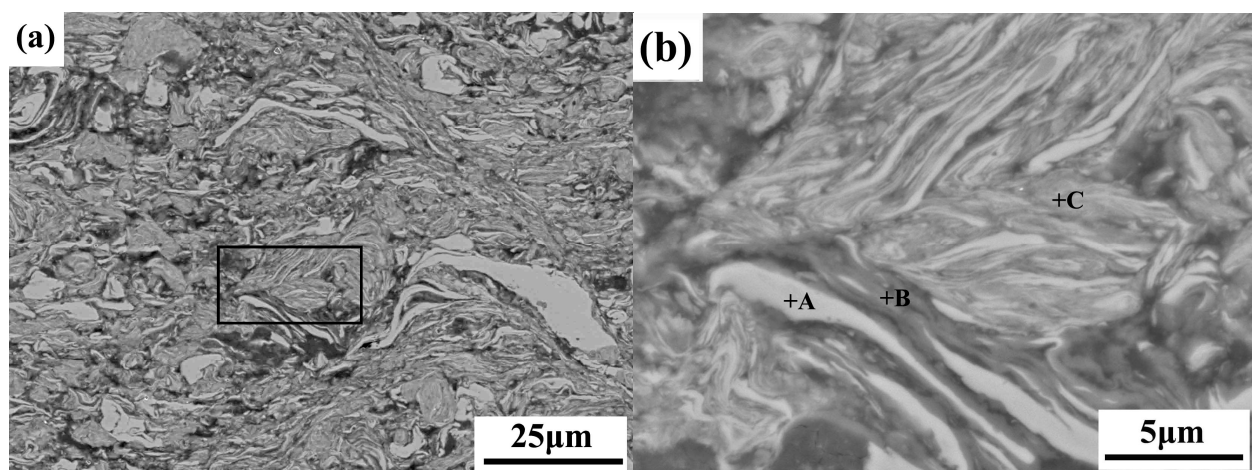


**Figure 2.** Backscattered SEM micrograph of the as-sprayed coating: (a) overview; (b) high magnification.

**Table 2.** EDS results of the three zones marked in Figure 2b.

Positions	Al K (at.%)	Fe K (at.%)
Point A	5.70	94.30
Point B	87.55	12.45
Point C	27.94	72.06

Figure 3 shows a TEM image of the as-sprayed Fe(Al) alloy coating. Typical grains observed in the coating had an equiaxed morphology with a grain size range of 10–50 nm. The corresponding selected area diffraction (SAD) pattern indicated a  $\alpha$ -Fe phase with a bcc structure. Therefore, a nanograin Fe(Al) alloy coating can be obtained through cold spraying of mechanically alloyed powder.

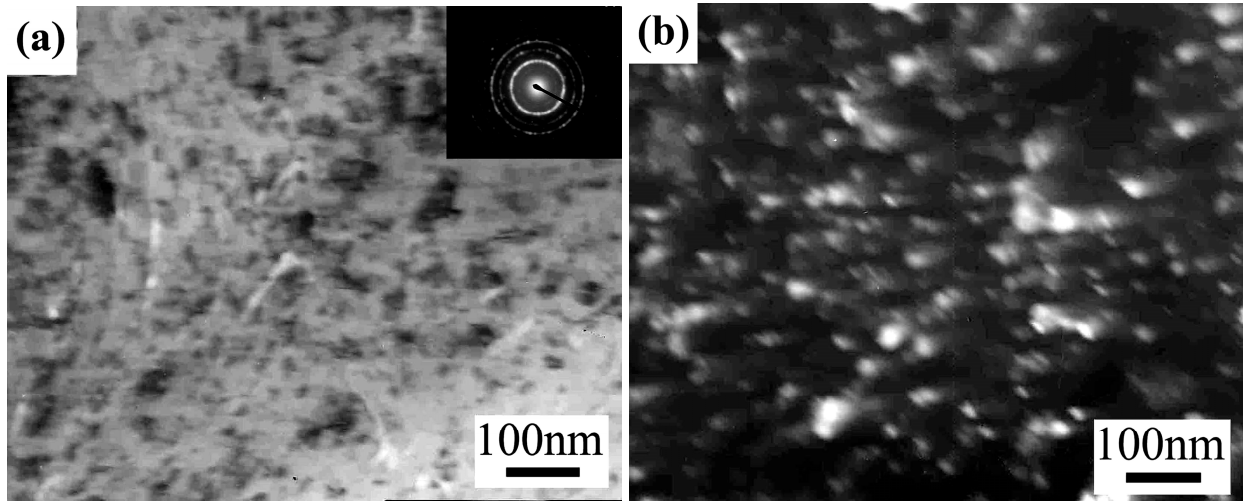


**Figure 3.** TEM micrograph of the as-sprayed coating: (a) bright-field and (b) dark-field.

### 3.2. Phase Structure Evolution during Annealing Treatment

From the XRD spectrum in Figure 4, the as-sprayed coating was mainly made up of  $\alpha$ -Fe(Al) solid solution phase and a trace of Al phase, which indicated that this coating was an Fe(Al) alloy not an FeAl intermetallic. After annealing at 500 °C for 5 h, the coating mainly consisted of FeAl intermetallic phase; however, Fe(Al) phase peaks with a very low height still can be found. This remnant Fe(Al) phase will completely transform to an FeAl intermetallic phase through increasing annealing time [20] or raising annealing temperature. After annealing at 700 °C for 5 h, the coating completely consisted of FeAl phase. By raising the temperature to 950 and 1050 °C, respectively, the phase structure of the deposit remained unchangeable and was still an FeAl intermetallic phase.

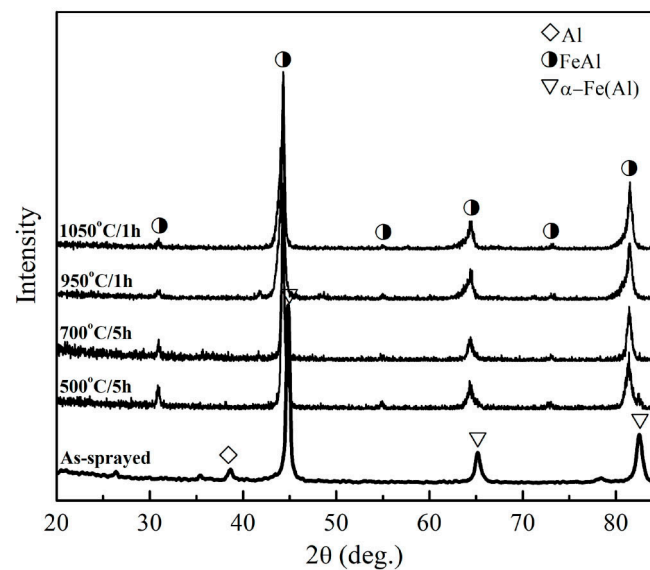


**Figure 4.** XRD patterns of as-sprayed and annealed coating.

### 3.3. Microstructure Evolution during Annealing Treatment

Backscattered SEM images of the microstructure of coatings annealed at 200 °C, 500 °C, 700 °C and 950 °C, respectively, are shown in Figure 5. It can be seen that after annealing at 200 °C, the coating microstructure had no obvious transformation compared to that of the as-sprayed coating. The lamellar structure in different contrast is still presented in the annealed coating, as marked by black arrows in Figure 5a, which indicates that elemental diffusion did not occur under this condition. This result was in agreement with the XRD analysis of the phase evolution of coating in a previous paper [20]. However, when raising the annealing temperature to 500 °C, the above-mentioned fine lamellar structure almost completely disappeared due to the high thermal reactivity and short diffusion distance of nanostructured FeAl coating. In addition, white Fe-rich zones (relatively thick layers) in the as-sprayed coating (Figure 2) became not obvious in contrast because of element diffusion within the coating, as shown in Figure 5b. This fact means that the heterogeneous feature in the as-sprayed coating can be modified through annealing treatment. The diffusion in the coating led to the elimination of micro-pores and the uniform distribution of elements. After annealing at 700 °C, the heterogeneous structure of elements completely disappeared, and the coating microstructure had been evidently improved. Furthermore, after annealing at 950 °C, the coating became very dense and homogeneous. Previous lamellar structures in the coating had totally vanished through interface diffusion. Therefore, coating microstructure homogenization was achieved through post-spray annealing treatment.

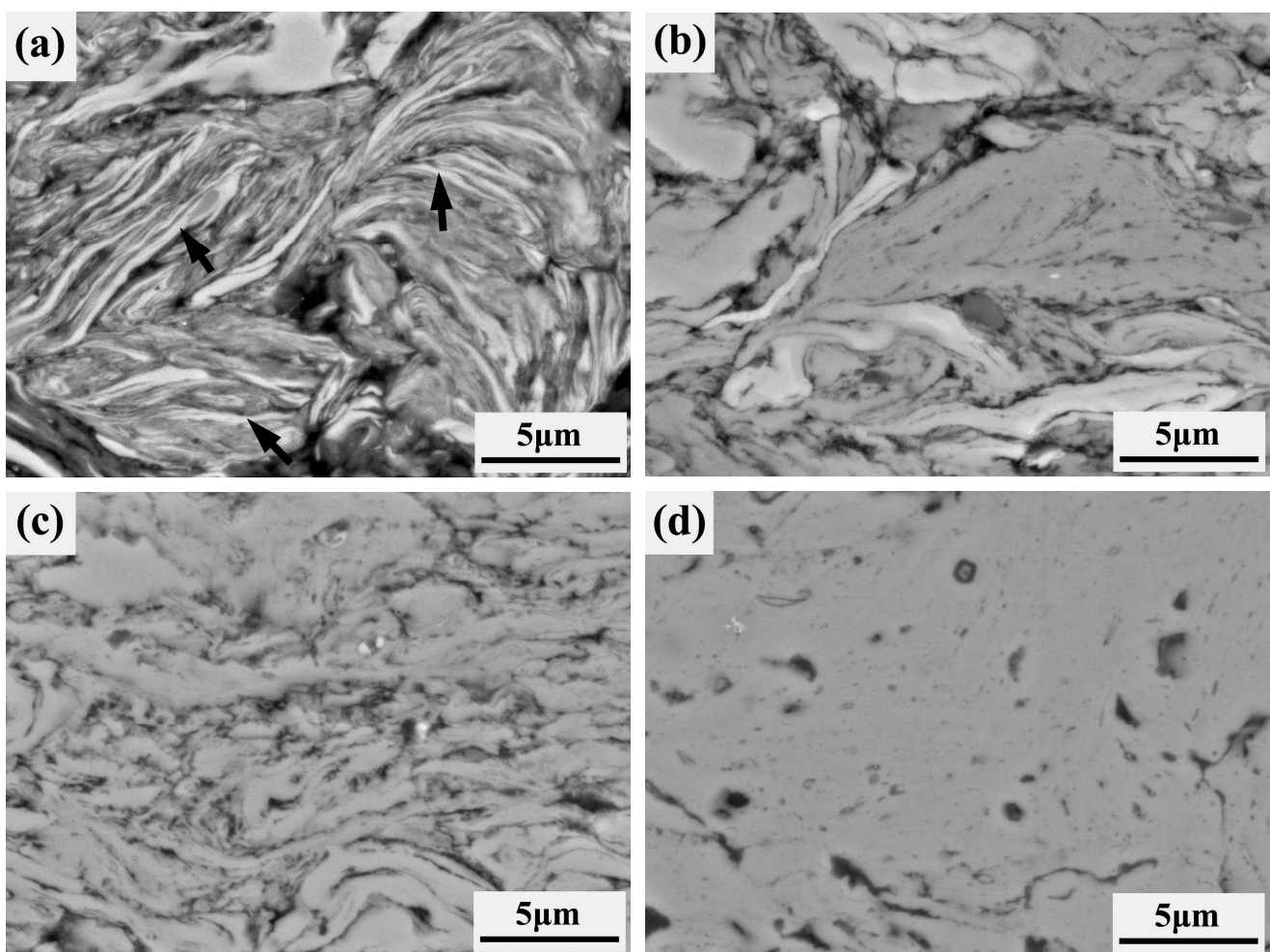


**Figure 5.** Backscattered SEM images of the coatings after annealing at (a) 200 °C, (b) 500 °C for 25 h and (c) 700 °C, (d) 950 °C for 5 h.

Figure 6 shows the results of TEM observations of FeAl coating after annealing at different temperatures. The coating annealed at 500 °C was made up of FeAl nanograin with an estimated size of between 10–50 nm [20]. After annealing at 700 °C for 5 h, the grain size in the coating exhibited a certain increase and was still less than 100 nm, as shown in Figure 6b. Generally, nanograin would rapidly grow as the annealing temperature rises. The enhanced thermal stability of nanocrystalline in the present FeAl coating involved two factors: the effect of solute drag [29] and Zener pinning [30] by oxide and grain boundary energy reduction, which was ascribed to aluminum atom segregation and structure ordering [31]. When increasing the temperature to 950 °C, the FeAl grain significantly grew and the grain size reached about 200 nm, as shown in Figure 6c. The change tendency of FeAl grain size with annealing temperature in the present coating was in agreement with the results observed by Morris et. Al. [32] in annealing milled nanostructured FeAl. They found that the grain size changed slightly at low temperatures and significantly increased at higher temperatures (above 900 °C). These facts suggest that nanograin in FeAl coating can be maintained up to a temperature of less than 950 °C.

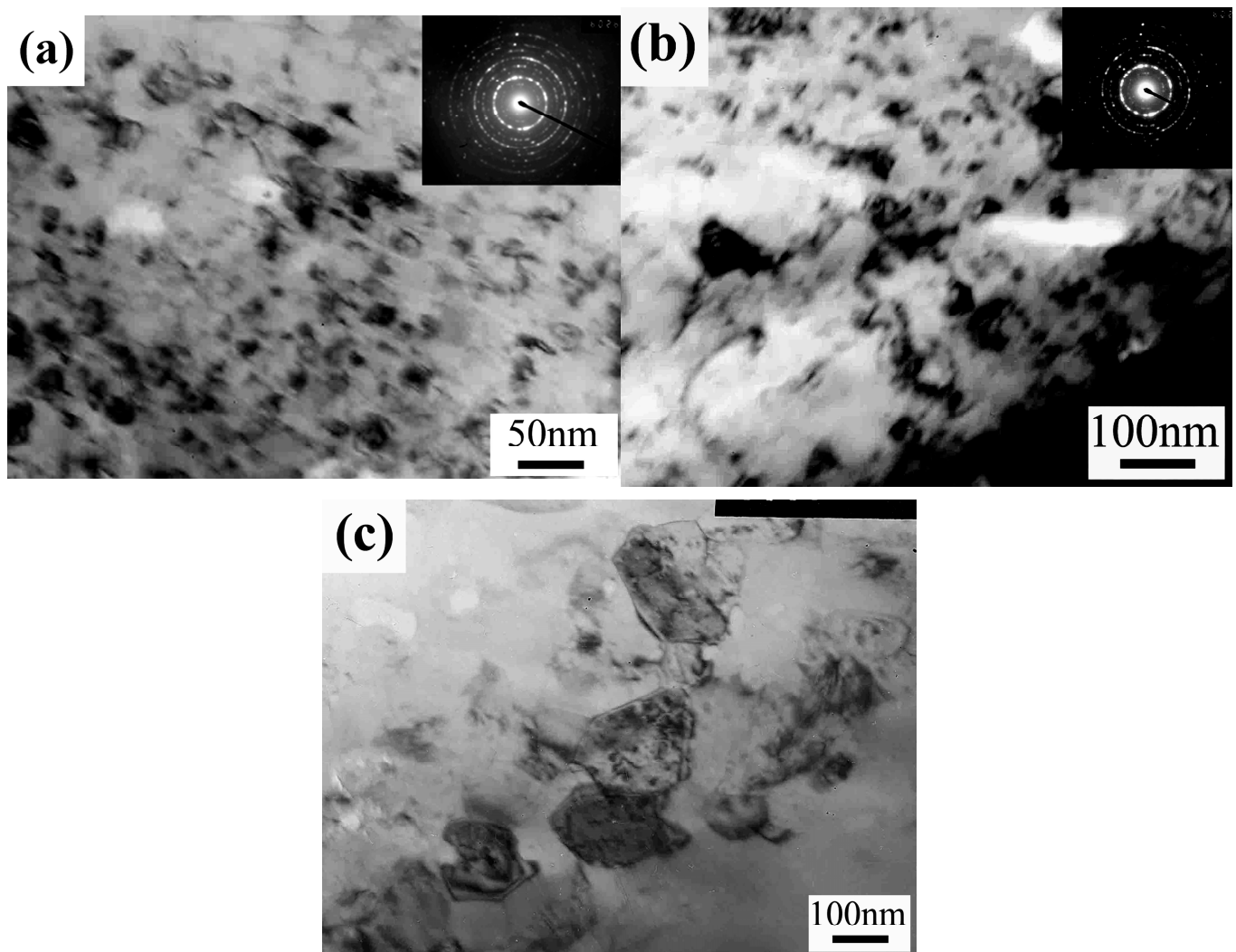


**Figure 6.** Bright-field TEM images of the nanocrystalline FeAl intermetallics after annealing at (a) 500 °C for 25 h, (b) 700 °C and (c) 950 °C for 5 h.

### 3.4. Microhardness Evolution during Annealing Treatment

Figure 7 presents the microhardness evolution of FeAl coating after annealing treatment [28]. Coating microhardness changed little and remained at about 400  $HV_{0.1}$  during annealing at temperatures below 800 °C. Such change can be attributed to the change in the FeAl coating microstructure. Only recovery and reordering occurred when annealing occurred within the temperature range of 100–250 °C, whereas recrystallization and grain growth would take place at elevated temperatures [33]. In the present study, as revealed by XRD analysis, the phase transformation from Fe(Al) alloy to FeAl occurred at an annealing temperature of 500 °C. The significant increase in grain size took place at a temperature from 700 to 950 °C. A significant decrease in coating microhardness at an annealing temperature from 800 to 900 °C is consistent with the occurrence of rapid grain growth as observed by TEM mentioned above. Therefore, the fact that annealing at 900 °C caused a significant decrease in the coating microhardness can be attributed to nanograin growth. Although the cohesion between the deposited particles was improved after annealing at 950 °C, as shown in Figure 5d, the strength of the FeAl coating would be lowered owing to the coarsening of the FeAl grain. With further raising of the annealing temperature to 1100 °C, coating microhardness changed little and had a microhardness of about 300  $HV_{0.1}$ , which was similar to that of the HVOF FeAl coating with coarse grains [9]. Therefore, the size control of FeAl grain through annealing of cold-sprayed nanostructured FeAl alloy can be of significant importance.

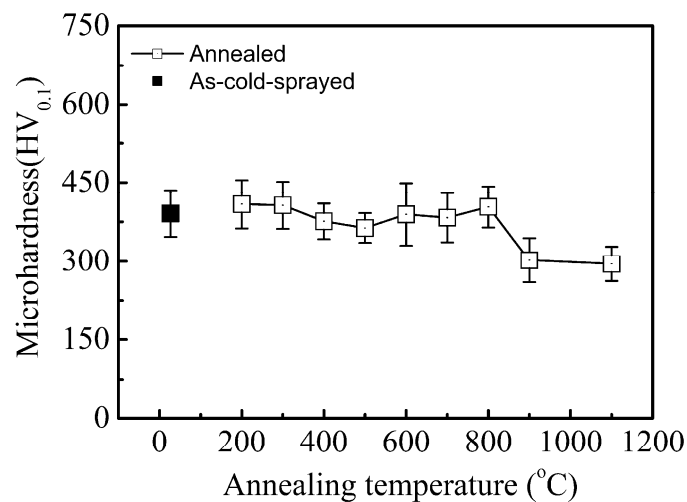


**Figure 7.** Microhardness evolution of FeAl coating with annealing temperature.

### 3.5. Wear Property Evolution during Annealing Treatment

Figure 8 shows friction coefficient (FC) curves of as-sprayed and annealed coatings. It can be seen that FC change curves of these coatings exhibited obvious fluctuations during the whole test process. For as-sprayed coating, its average FC gradually reached a steady state at about 0.8 after experiencing a running-in period of about 12 min, which then remained steady during the rest of the test. However, the FC of FeAl coating annealed at 700 °C increased continuously during the whole test duration and its maximum even reached about 1.4, which could be associated with the high adhesive contact between the  $Si_3N_4$  ball and the coating material due to a great deal of wear debris. The FC of FeAl coatings annealed at 950 °C and 1050 °C showed comparatively similar wear behavior, namely, there was a sharp increase in the early minutes, and then the FC rapidly reached a relatively steady state at about 1.04 and 1.08, respectively, which remained unchangeable during the rest of the test except for a little local fluctuation.

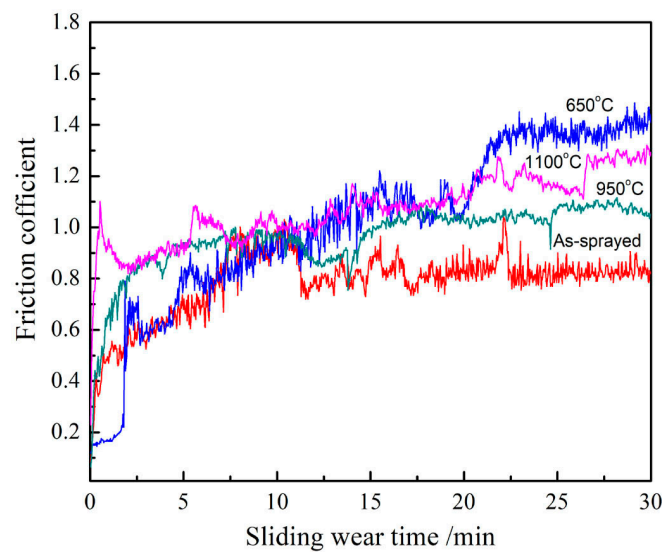


**Figure 8.** Evolution of friction coefficient versus sliding time for as-sprayed and annealed FeAl coatings.

Considering the basically similar microhardness of these coatings (in Figure 7), different friction coefficients would be mainly related to their microstructure characteristics (in Figure 5) and wear mechanism, which can be explained through the observation of wear track morphology. Figure 9 shows the SEM morphologies of the worn tracks of different coatings with 10 N load after sliding 90 m. The magnitudes of their respective wear widths as well as the wear volume loss and the calculated wear rates are shown in Table 3. It can be seen that FeAl coating annealed at 700 °C presented the widest wear track and the roughest morphology, whereas FeAl coatings annealed above 950 °C exhibited the narrowest wear track and the smoothest wear surface, as shown in Figure 9a–d, which was in agreement with the wear test results in Table 3. This fact indicates that FeAl coating annealed at a temperature above 950 ° will have significantly improved wear resistance, which can be attributed to the enhanced cohesion strength between inter-splats (in Figure 5).

**Table 3.** Wear track features of different coatings.

	As-Sprayed	650 °C	950 °C	1100 °C
Friction coefficient	0.82	1.13	1.05	1.08
Wear track width/ $\mu\text{m}$	$1102 \pm 68$	$1717 \pm 46$	$552 \pm 11$	$569 \pm 58$
Wear volume/ $\text{mm}^3$	$16.5 \times 10^{-2}$	$79.5 \times 10^{-2}$	$8.5 \times 10^{-3}$	$6.5 \times 10^{-3}$
Wear rate/ $\text{mm}^3 \cdot \text{N}^{-1} \cdot \text{m}^{-1}$	$1.8 \times 10^{-4}$	$8.8 \times 10^{-4}$	$9.4 \times 10^{-6}$	$7.2 \times 10^{-6}$

From the high magnification SEM images in Figure 9e,f, it can be seen that as-sprayed Fe(Al) alloy coating and annealed FeAl coating at 700 °C showed similar wear behavior. A thick oxide layer, local cracks and a peeled-off oxide layer can be observed on the worn surface of coatings. As a result, these two coatings exhibited a high wear rate in the order of magnitude range of  $10^{-4}$  (as indicated in Table 3). It was noticeable that FeAl coating obtained after annealing at 700 °C presented a higher wear rate compared to as-sprayed Fe(Al) alloy, which would be related to its intrinsic brittleness [2] and not-fully improved inter-splat bonding strength (as indicated in Figure 5b). Therefore, oxidation and oxide layer fragment were the main wear mechanisms of these two coatings. Generally, friction heating induced by contacting asperities between the ball and FeAl material during the dry sliding wear process, would cause a high interface temperature, which correspondingly resulted in material oxidation. Figure 10 provides SEM images of the worn surface of as-sprayed coating and the corresponding EDS spectrum. A large number of adhered oxide layers can be easily found on the worn surface due to an intensive friction heating effect. EDS analysis of different points on

the worn track indicated that the worn surface was mainly composed of Fe, Al and O. Therefore, iron and aluminum oxides existed in the worn surface of the coating. These adhered oxide layers, which were considered to act as a solid lubricant [34], can reduce adhesion between the  $\text{Si}_3\text{N}_4$  ball and FeAl coating to a certain extent, thus decreasing the friction coefficient. Therefore, as-sprayed Fe(Al) alloy exhibited the lowest FC (as shown in Table 3). However, on the other hand, shear stress occurring at the oxide layer due to contact stress would accelerate the initiation and propagation of cracks and finally result in the overall detachment of the thicker oxide layer, as shown in Figure 9e,f. To sum up, these two coatings showed a high wear rate, as shown in Table 3.

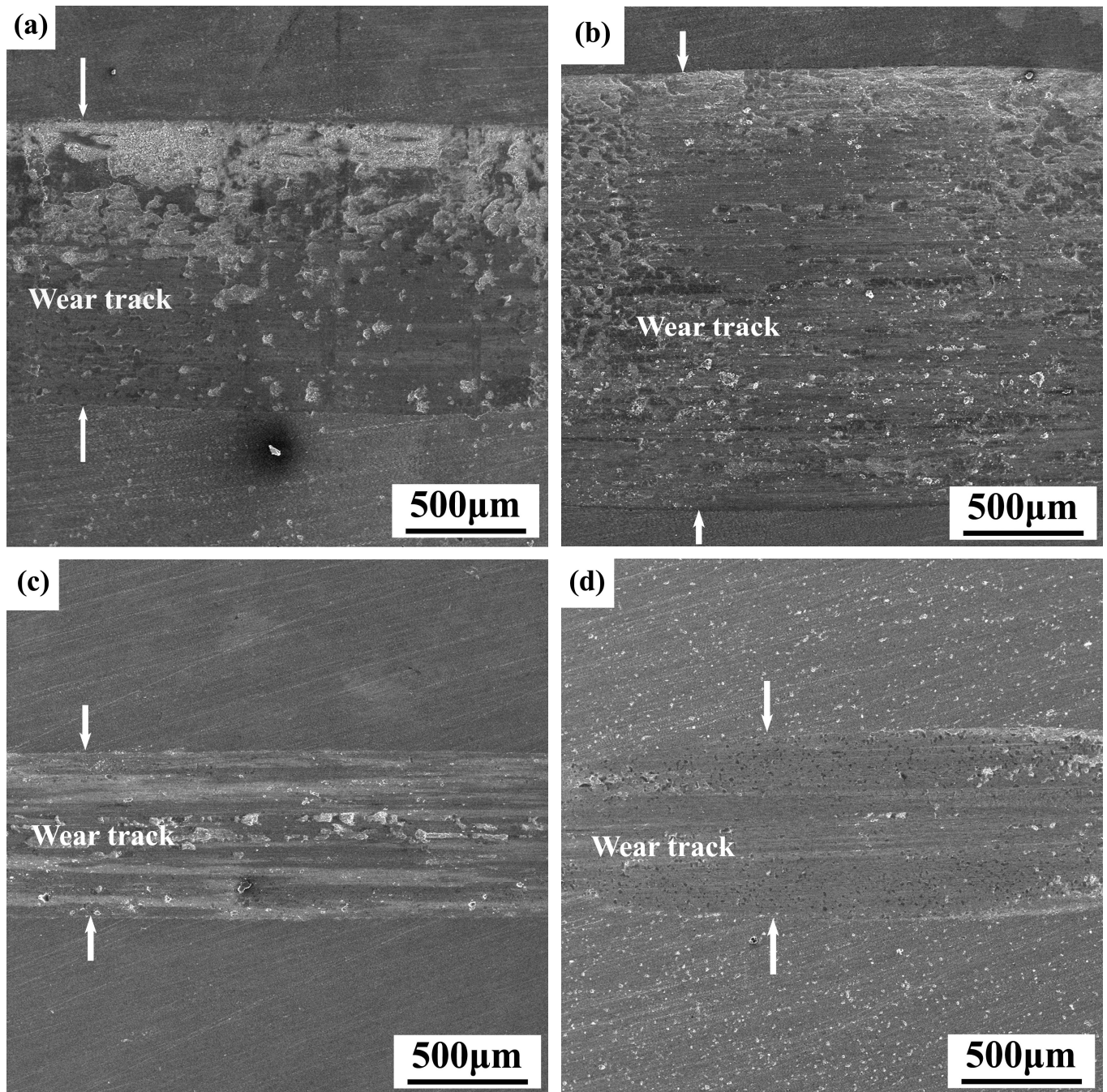
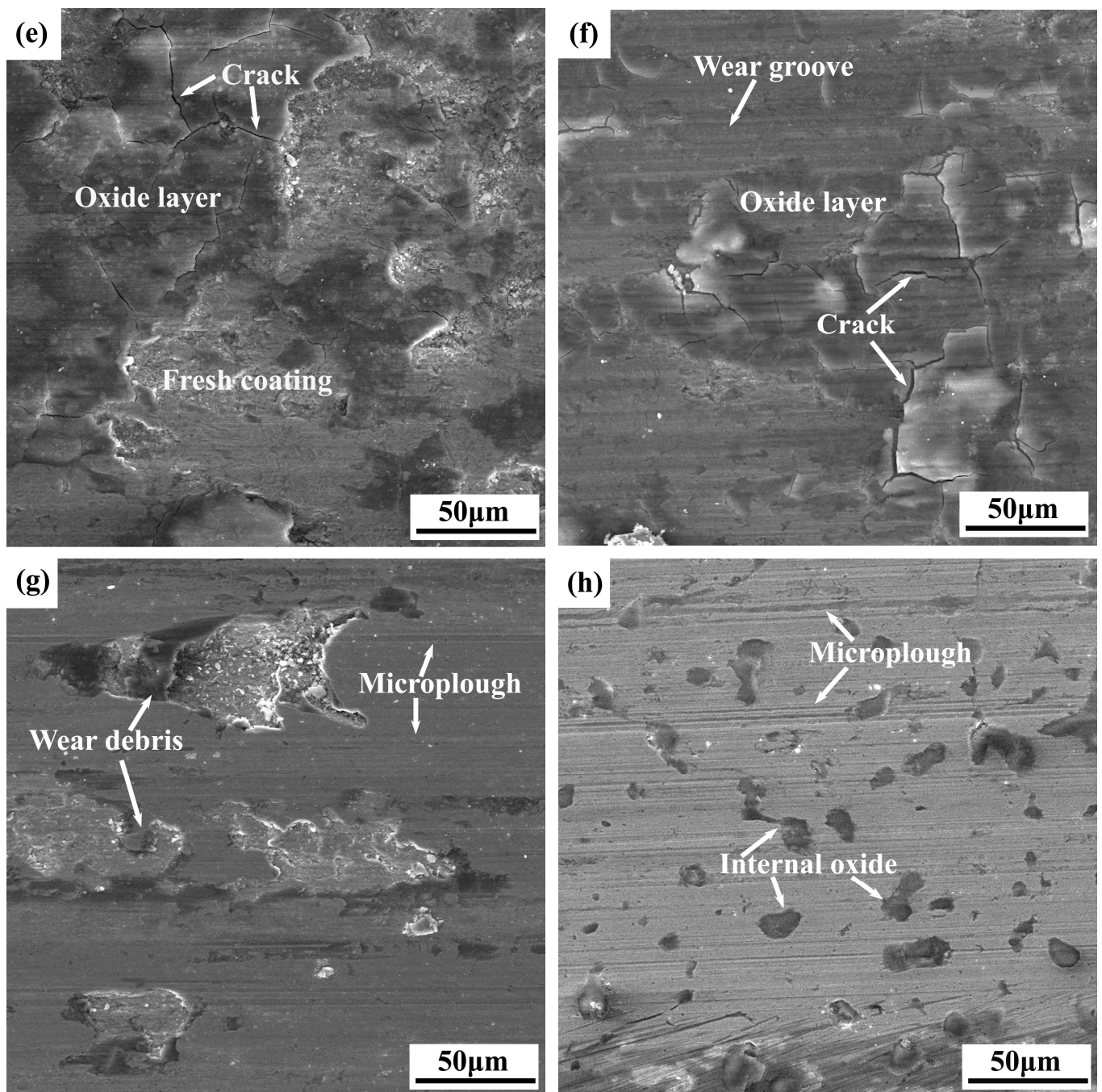


Figure 9. Cont.



**Figure 9.** SEM morphologies of the worn coatings: as-sprayed (a,e); annealed at 700 °C (b,f), 950 °C (c,g), 1050 °C (d,h), respectively.

From the high magnification SEM images in Figure 9g,h, it can be seen that FeAl coating annealed at 950 °C and 1050 °C showed similar wear behavior. Only a trace of grooves of micro-cutting and micro-cracks appeared on the worn surface with no obvious oxide layer fragment except for some plate-like debris. Therefore, these two coatings showed a very low wear rate in the order of magnitude range of  $10^{-6}$ . Generally, the adhesion strength between inter-splats in cold-sprayed coatings was low because of its lamellar structure and mechanical bonding. However, their mechanical properties can be significantly improved through annealing treatment [21–26]. In the present paper, the adhesion state between inter-splats in FeAl coating can be significantly improved by solid element diffusion after annealing at a high temperature of 950 °C (as indicated in Figure 5d). Consequently, the fracture and detachment of the oxide layer can be strongly restrained

during the sliding wear process, and these two FeAl coatings exhibited a very low wear rate in spite of their decreased microhardness.

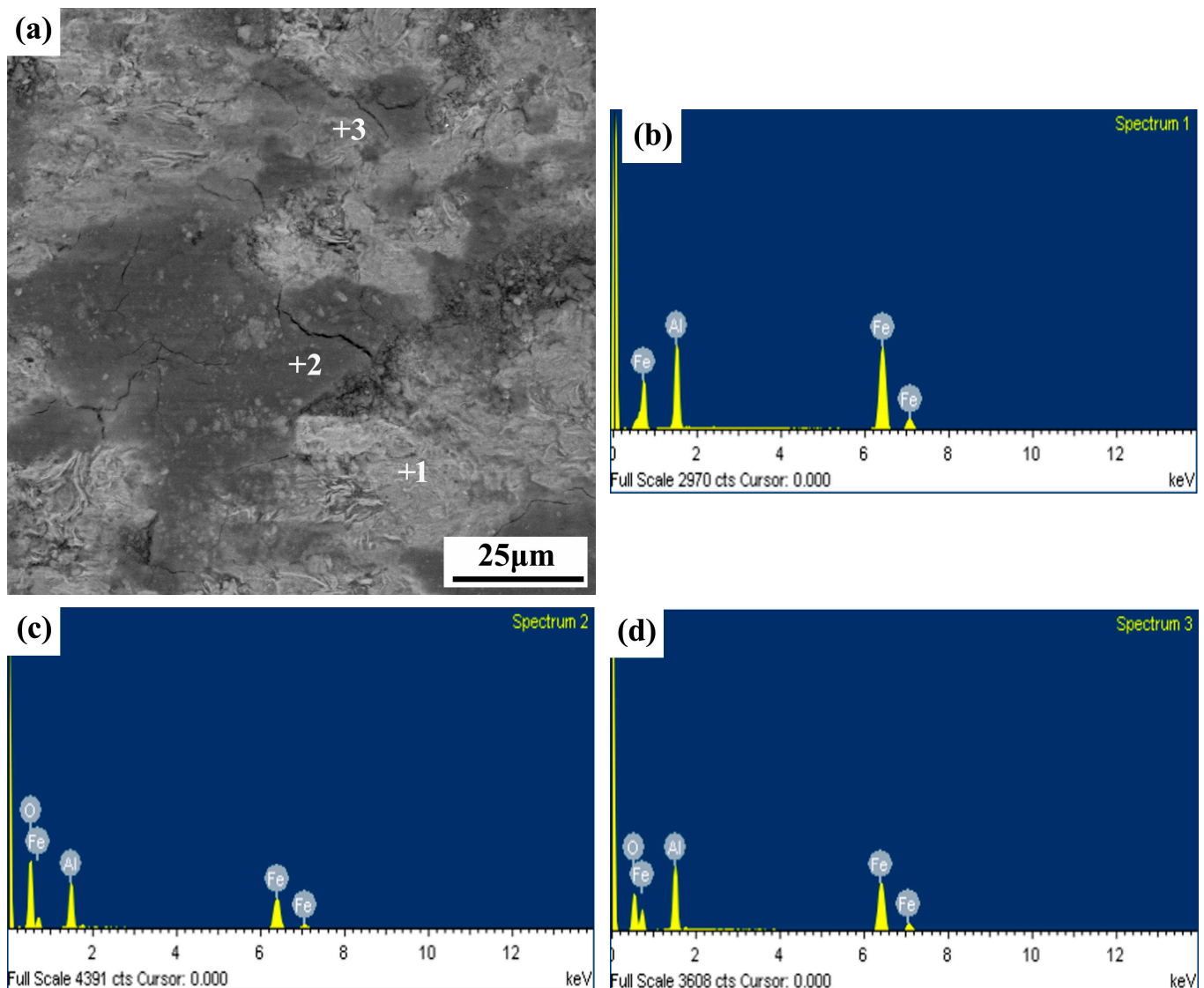


**Figure 10.** SEM image (a) of the worn track of as-sprayed coating and corresponding EDS results (b–d) in specific area.

#### 4. Conclusions

The effect of annealing treatment on the microstructure, phase structure, microhardness and dry sliding wear property of cold-sprayed nanostructured FeAl coating was investigated. It was found that annealing treatment provided an effective approach to control the microstructure, microhardness and wear property of the cold-sprayed FeAl coating. After annealing at a temperature less than 700 °C, minimal grain growth of the FeAl nanograin was observed accompanied by an improvement in the microstructure of the cold-sprayed coating at elevated treatment temperatures. The microhardness of the cold-sprayed FeAl coating remained at about 400 Hv<sub>0.1</sub> when annealed at temperatures below 800 °C and decreased significantly with increasing annealing temperature up to 900 °C, which may be attributed to the grain growth of the FeAl nanograin and the softening of the matrix during annealing treatment. Dry sliding wear tests showed that as-sprayed Fe(Al) alloy coating and obtained FeAl intermetallic coating after annealing at 700 °C were worn by delamination of the oxide layer and showed the high wear rate. In contrast, FeAl coatings annealed at 950 °C and 1050 °C almost did not suffer from oxide

layer fragmentation except for little grooves that resulted from microploughing. Therefore, these two FeAl coatings exhibited a very low wear rate in the order of magnitude range of  $10^{-6}$ .

**Author Contributions:** Conceptualization, H.W. and F.A.; methodology, H.W., X.B. and H.Y.; software, M.Z. and Q.C.; validation, H.W., F.A., H.Y. and Q.C.; formal analysis, H.W., F.A. and G.J.; investigation, F.A., X.B. and M.Z.; resources, H.W. and F.A.; data curation, H.W., F.A. and X.B.; writing—original draft preparation, H.W., F.A. and X.B.; writing—review and editing, H.W. and C.S.R.; visualization, H.W. and C.S.R.; supervision, H.W.; project administration, H.W.; funding acquisition, H.W. All authors have read and agreed to the published version of the manuscript.

**Funding:** The authors thank for the financial support from the National Natural Science Foundation of China (No.51001056 and 52161012) and the Natural Science Foundation of Jiangxi Province (No.20192BAB206006).

**Institutional Review Board Statement:** Not applicable.

**Informed Consent Statement:** Not applicable.

**Data Availability Statement:** All data that support the findings of this study are included within the article.

**Conflicts of Interest:** The authors declare no conflict of interest.

## References

1. Tortorelli, P.F.; Natesan, K. Critical factors affecting the high-temperature corrosion performance of iron aluminides. *Mater. Sci. Eng. A* **1998**, *258*, 115–125. [[CrossRef](#)]
2. Stoloff, N.S. Iron Aluminides: Present status and future prospects. *Mater. Sci. Eng. A* **1998**, *258*, 1–14. [[CrossRef](#)]
3. McKamey, C.G.; DeVan, J.H.; Tortorelli, P.F.; Sikka, V.K. A review of recent developments on Fe<sub>3</sub>Al-based alloys. *J. Mater. Res.* **1991**, *6*, 1779–1805. [[CrossRef](#)]
4. Alman, D.E.; Hawk, J.A.; Tylczak, J.H.; Dogan, C.P.; Wilson, R.D. Wear of iron-aluminide intermetallic-based alloys and composites by hard particles. *Wear* **2001**, *251*, 875–884. [[CrossRef](#)]
5. Deevi, S.C.; Sikka, V.K.; Processing, C.T.L. Properties, and applications of nickel and iron aluminides. *Prog. Mater. Sci.* **1997**, *42*, 177–192. [[CrossRef](#)]
6. McFadden, S.X.; Mishra, R.S.; Valiev, R.Z.; Zhilyaev, A.P.; Mukherjee, A.K. Mukherjee: Low-temperature superplasticity in nanostructured nickel and metal alloys. *Nature* **1999**, *398*, 684–686. [[CrossRef](#)]
7. Kumar, S.; Selvarajan, V.; Padmanabhan, P.V.A.; Sreekumarand, K.P. Characterization and comparison between ball milled and plasma processed iron-aluminium thermal spray coatings. *Surf. Coat. Technol.* **2006**, *201*, 1267–1275. [[CrossRef](#)]
8. Hearley, J.A.; Little, J.A.; Sturgeon, A.J. The effect of spray parameters on the properties of high velocity oxy-fuel NiAl intermetallic coatings. *Surf. Coat. Technol.* **2000**, *123*, 210–218. [[CrossRef](#)]
9. Ji, G.; Grosdidier, T.; Liao, H.L.; Morniroli, J.P.; Coddet, C. Spray forming thick nanostructured and microstructured FeAl deposits. *Intermetallics* **2005**, *13*, 596–607. [[CrossRef](#)]
10. Wang, H.T.; Ji, G.C.; Li, C.J. Characterization of microstructure and properties of nanostructured Fe-Al/WC intermetallic composite coating deposited by cold spraying. In Proceedings of the 2010 International Conference on Mechanic Automation and Control Engineering, Wuhan, China, 26–28 June 2010.
11. Ajdelsztajn, L.; Jodoin, B.; Schoenung, J.M. Synthesis and mechanical properties of nanocrystalline Ni coatings produced by cold gas dynamic spraying. *Surf. Coat. Technol.* **2006**, *201*, 1166–1172. [[CrossRef](#)]
12. Shukla, V.; Elliott, G.S.; Kear, B.H.; McCandlish, L.E. Hyperkinetic deposition of nanopowders by supersonic rectangular jet impingement. *Scr. Mater.* **2001**, *44*, 2179–2182. [[CrossRef](#)]
13. Li, C.-J.; Li, W.Y. Deposition characteristics of titanium coatings in cold spraying. *Surf. Coat. Technol.* **2003**, *167*, 278–283. [[CrossRef](#)]
14. Morelli, D.T.; Elmoursi, A.A.; Van Steenkiste, T.H.; Gorkiewicz, D.W.; Gillispie, B. Kinetic spray of aluminum metal matrix composites for thermal management applications. In *Thermal Spray 2003: Advancing the Science and Applying the Technology*; Marple, B.R., Moreau, C., Eds.; ASM International: Materials Park, OH, USA, 2003; pp. 85–90.
15. Van Steenkiste, T.H.; Elmoursi, A.; Gorkiewicz, D.; Gillispie, B. Fracture study of aluminum composite coatings produced by the kinetic spray method. *Surf. Coat. Technol.* **2005**, *194*, 103–110. [[CrossRef](#)]
16. Li, W.-Y.; Zhang, G.; Zhang, C.; Elkedim, O.; Liao, H.; Coddet, C. Effect of ball milling of feedstock powder on microstructure and properties of TiN particle-reinforced Al alloy-based composites fabricated by cold spraying. *J. Therm. Spray Technol.* **2008**, *17*, 316–322. [[CrossRef](#)]
17. Lima, R.S.; Karthikeyan, J.; Kay, C.M.; Lindemann, J.; Berndt, C.C. Microstructural characteristics of cold-sprayed nanostructured WC-Co coatings. *Thin Solid Film.* **2002**, *416*, 129–135. [[CrossRef](#)]

18. Kim, H.J.; Lee, C.H.; Hwang, S.Y. Superhard nano WC-12%Co coating by cold spray deposition. *Mater. Sci. Eng. A* **2005**, *391*, 243–248. [[CrossRef](#)]
19. Gao, P.H.; Li, C.-J.; Yang, G.J.; Li, Y.G.; Li, C.X. Influence of substrate hardness transition on built-up of nanostructured WC-12Co by cold spraying. *Appl. Surf. Sci.* **2010**, *256*, 2263–2268. [[CrossRef](#)]
20. Wang, H.T.; Li, C.-J.; Yang, G.J.; Li, C.X.; Zhang, Q.; Li, W.Y. Microstructural characterization of cold-sprayed nanostructured FeAl intermetallic compound coating and its ball-milled feedstock powders. *J. Therm. Spray Technol.* **2007**, *16*, 669–676. [[CrossRef](#)]
21. Wang, H.T.; Li, C.-J.; Yang, G.J.; Li, C.X. Effect of heat treatment on the microstructure and property of cold-sprayed nanostructured FeAl/Al<sub>2</sub>O<sub>3</sub> intermetallic composite coating. *Vacuum* **2008**, *83*, 146–152. [[CrossRef](#)]
22. Li, W.Y.; Li, C.-J.; Liao, H.L. Effect of annealing treatment on the microstructure and properties of cold-sprayed Cu coating. *J. Therm. Spray Technol.* **2006**, *15*, 206–211. [[CrossRef](#)]
23. Borchers, C.; Gärtner, F.; Stoltenhoff, T.; Kreye, H. Formation of persistent dislocation loops by ultra-high strain-rate deformation during cold spraying. *Acta Mater.* **2005**, *53*, 2991–3000. [[CrossRef](#)]
24. Decker, M.K.; Neiser, R.A.; Gilmore, D.; Tran, H.D. Microstructure and properties of cold spray nickel. In *Thermal Spray 2001: New Surfaces for a New Millennium, Proceedings of the International Thermal Spray Conference, Singapore, 28–30 May 2001*; Berndt, C.C., Khor, K.A., Lugscheider, E.F., Eds.; ASM International: Materials Park, OH, USA, 2001; pp. 433–439.
25. McCune, R.C.; Donlon, W.T.; Popoola, O.O.; Cartwright, E.L. Characterization of copper layers produced by cold gas-dynamic spraying. *J. Therm. Spray Technol.* **2000**, *9*, 73–82. [[CrossRef](#)]
26. Li, W.Y.; Guo, X.P.; Verdy, C.; Dembinski, L.; Liao, H.L.; Coddet, C. Improvement of microstructure and property of cold-sprayed Cu-4 at.%Cr-2 at.%Nb alloy by heat treatment. *Scr. Mater.* **2006**, *55*, 327–330. [[CrossRef](#)]
27. Li, C.-J.; Wang, H.T.; Yang, G.J.; Bao, C.G. Characterization of high-temperature abrasive wear of cold-sprayed FeAl intermetallic compound coating. *J. Therm. Spray Technol.* **2011**, *20*, 227–233. [[CrossRef](#)]
28. Wang, H.T.; Li, C.-J.; Yang, G.J. Influence of hard phase on the properties of cold-sprayed FeAl intermetallic compound coatings. *Mater. Prot.* **2010**, *43*, 93–94. (In Chinese)
29. Knauth, P.; Charai, A.; Gas, P. Grain growth of pure nickel and of a Ni-Si solid solution studied by differential scanning calorimetry on nanometer-sized crystals. *Scr. Metall. Mater.* **1993**, *28*, 325–330. [[CrossRef](#)]
30. Boylan, K.; Ostrander, D.; Erb, U.; Palumbo, G.; Aust, K.T. An in-situ TEM study of the thermal stability of nanocrystalline Ni. *Scr. Metall. Mater.* **1991**, *25*, 2711–2716. [[CrossRef](#)]
31. Gao, Z.; Fultz, B. The thermal stability of nanocrystalline Fe-Si-Nb prepared by mechanical alloying. *Nanostruct. Mater.* **1993**, *2*, 231–240. [[CrossRef](#)]
32. Morris, D.G.; Gutierrez-Urrutia, I.; Munoz-Morris, M.A. Hardening and softening in milled nanostructured FeAl on annealing. *Scr. Mater.* **2007**, *57*, 369–372. [[CrossRef](#)]
33. Gialanella, S.; Amils, X.; Barò, M.D.; Delcroix, P.; Le Caër, G.; Lutterotti, L.; Suriñac, S. Microstructural and kinetic aspects of the transformations induced in a FeAl alloy by ball-milling and thermal treatments. *Acta Mater.* **1998**, *46*, 3305–3316. [[CrossRef](#)]
34. Stott, F.H.; Glascott, J.; Wood, G.C. The sliding wear of commercial Fe-12%Cr alloys at high temperature. *Wear* **1985**, *101*, 311–324. [[CrossRef](#)]

**Disclaimer/Publisher’s Note:** The statements, opinions and data contained in all publications are solely those of the individual author(s) and contributor(s) and not of MDPI and/or the editor(s). MDPI and/or the editor(s) disclaim responsibility for any injury to people or property resulting from any ideas, methods, instructions or products referred to in the content.